Fabrication of paper-based microfluidic devices using a 3D printer and a commercially-available wax filament

Antonio Espinosa,

Joannes Diaz,

Edgar Vazquez,

Lina Acosta,

Arianna Santiago,

Lisandro Cunci[*]

Department of Chemistry, Universidad Ana G. Méndez – Recinto de Gurabo, Carr. 189, Km 3.3, Gurabo, Puerto Rico 00778, United States

Abstract

In this work, we developed an alternative manufacturing paper-based microfluidics method through 3D printing and wax filament. Microfluidic paper-based analytical devices (µPADs) are low-cost and easy-to-manufacture tools used for various chemical and biological analyses and studies. Paper-based microfluidics with wax has been limited as the manufacturers have discontinued most wax printing equipment. We aim to develop a low-cost and accessible manufacturing method that can replace conventional wax-on paper-based microfluidic manufacturing methods. Using highly available commercial 3D printing technology and wax filament, we could create hydrophobic wax barriers on the surface of different paper types. The properties and limits of this manufacturing method were characterized. Moreover, using this paper-based microfluidic manufacturing method, we were able to measure dopamine electrochemically using µPAD as a passive flow-based method in concentrations as low as 1 nM using injections as small as 15 µL.

Keywords

Microfluidic paper-based analytical devices; Wax filament; 3D printer; Passive flow

---

[*]Corresponding author. cuncil1@uagm.edu (L. Cunci).

1. Introduction

The use of microfluidics has become an essential tool for micro-and nano-scale chemical analysis and biological studies. This technology allows minimal amounts of flow in a minimum quantity of liquid or sample flow with microfluidic systems to perform biosensing [1]. Microfluidic systems can be characterized as active or passive, depending on the force applied to the sample or flow. While active microfluidic devices require pumps to move the fluid through the channels, passive flow microfluidic systems use the chemical and physical properties of the channels to move the fluids. Among the passive microfluidic systems, microfluidic paper-based analytical devices, also known as µPADS, are one of the most promising systems due to their manufacture and operating feasibility, they are cost-effective, and they use very low sample volume [2–5].

Furthermore, µPADS are the most widely used and highly suitable for point-of-care testing thanks to their ability to passively move the flow due to capillarity and portability [6–9]. The detection limit and resolution of µPADS depend significantly on the method used to detect an analyte of interest in human body fluids such as saliva, tears, and sweat. The most common detection methods are colorimetric, fluorescent, chemiluminescent, and electrochemical assays [10]. Nowadays, most developed µPADS rely on colorimetric detection as it is easy to use, and data interpretation is very simple [11]. However, this detection method suffers from poor sensitivity, very small linear ranges or high detection limits, and colorimetric reactions are often difficult to detect at low concentrations. With the use of electrochemical detection methods, the sensitivity and selectivity of the µPADS can be improved over naked eye detection without jeopardizing portability and quality [11].

Morbioli et al. [12] published an article developing a microfluidic manufacturing method in Polydimethylsiloxane (PDMS). They combined printed wax molds using a Xerox™ Phaser 8580 wax printer. Younas et al. [13] developed a microfluidic paper-based analytic devices (µPAD) manufacturing technique to analyze milk adulteration. This group manufactured µPAD on Grade 1 filter paper using a Xerox ColorQube 8580 Printer. Nilghaz et al. [14] developed a fabric-based microfluidic device by wax printing. This group used a Xerox ColorQube 8570 wax printer to print solid wax on cotton, silk, and polyester fabrics. However, this type of solid wax printer has been discontinued, and those who depend on a wax printer to make paper-based microfluidics are limited to the lifespan of the printers they currently own or those models that they still sell in used condition. There is a great need to develop new methods of manufacture of paper-based microfluidics that are open-source with the potential to be scalable and widely available for the scientific community.

Chiang et al. [15] published an article developing a method of manufacturing µPADS for glucose and nitrite assays using a 3D printer and paraffin wax. This group used a modified Prusa i3 3D printer with a custom-designed extrusion print head consisting of a syringe pump, PMMA frame, a stepper motor, piston, and a thermistor probe to dispense molten wax onto a paper surface [15]. This method of manufacturing µPADS through 3D printing required engineering, coding, and machine learning skills, which limited the accessibility of this manufacturing technique since it requires engineering professionals and knowledge of Arduino programming. In this work, we aimed to develop a µPADS manufacturing method

using a commercial 3D printer and wax filament. Our μPADS manufacturing method is low cost, easy, and accessible to anyone with a 3D printer and commercially available wax filament without any modifications to the 3D printer.

One of the applications of great interest is to use paper-based microfluidics as a passive flow method for flexible biosensors that can be worn in the human body as wearable technology. Given the complexity of the structure of some electronics and the high manufacturing cost, lightweight and flexible materials such as paper are being used to improve some current sensor devices [16]. For developing this type of flexible biosensors, flexible and planar electrodes are usually used to monitor a particular analyte constantly. One of the most common flexible and planar electrodes are inkjet printed electrodes. This type of electrode is manufactured by printing a pattern on the surface of a flexible substrate with conductive inks such as silver, copper, and carbon nanotube conductive inks. Inkjet printing electrodes today is a very popular technique due to its low manufacturing cost. Unlike methods such as screen printing, inkjet-printed electrodes do not require prefabrication of a template or stencil since the pattern is designed in software and sent directly to the printer, which deposits drops of ink to form the desired shape [17]. To test the effectiveness of our μPADS manufacturing method through 3D printing and wax filament, we performed an electrochemical assay and selected dopamine as a model biomolecule. Dopamine is a well-known studied neurotransmitter and is associated with diseases such as Parkinson's disease. Dopamine can be found in body fluids with a clinical range of 0 – 0.25 nM in blood and 0.3 – 3 μM in urine, and the clinical range of dopamine in sweat is currently being studied [18]. Moreover, basal concentration of dopamine in the brain is ca. 20 nM [19]. Recently, our research group measured dopamine through Electrochemical Impedance Spectroscopy (EIS) in concentrations as low as 1 nM using carbon microelectrodes [20]. Also, Lei et al. [21] developed a low-cost method to detect dopamine using single atom doping of $MoS2$ with manganese. With this flexible electrochemical device, they could detect dopamine concentrations in serum, urine, artificial sweat, and buffer with a detection limit of 50 pM in buffer solution, 5 nM in 10% serum, and 50 nM in artificial sweat [21].

2. Materials and methods

2.1. Reagents

GE Healthcare Life Science (Sigma-Aldrich) Whatman chromatography paper grade 1 (1 CHR) with a thickness of 0.18 mm was used as the primary material for the manufacture of microfluidic paper-based analytical devices (μPADS). This chromatography paper's linear flow rate (water) is 130 mm/30 min. Other papers tested were delicate task wipes (Kimwipes®, Kimberly-Clark Professional μPAD prototype. Briefly, tris buffer was prepared with 0.112 g of KCl, 4.33 g NaCl, 0.103 g $CaCl_2$•2 H_2O, 0.0815 g $MgCl_2$•6 H_2O, 0.107 g Na_2PO_4•7 H_2O, 0.0135 g Na_2PO_4• 2 H_2O, and 0.3029 g of tris for a quantity of 500 mL of solution. All reagents were purchased from Sigma-Aldrich. For the dopamine detection experiment by chronoamperometry, the dopamine solutions were prepared with PBS buffer at pH 7.4. PBS buffer was prepared with 8.008 g NaCl, 0.2013 g KCl, 1.7799 g Na_2HPO_4• 2 H_2O, and Na_2HPO_4•7 H_2O for a 1.0 L of solution. All reagents for the

PBS preparation and dopamine hydrochloride ($(HO)_2C_6H_3CH_2CH_2NH_2 \bullet HCl$) were also purchased from Sigma-Aldrich.

2.2. Wax 3D printing

Patterns were designed in Fusion 360 Academic Version (Autodesk). A Snapmaker 3D printer was used with a Moldlay wax filament to print all the designs shown in this work. Our 3D printer was set up with a nozzle diameter of 0.4 mm. After 3D printing, a laboratory oven was used at a constant temperature, which was characterized to find the optimal conditions. To deposit wax on the surface of the chromatography paper, a Moldlay filament with a 1.75 mm diameter was used. One-layer-height patterns were designed, and the .stl file was entered into the Snapmaker software, which generated the G-code to perform the 3D printing. All files in this work are available for free upon request. The G-code settings for the printing were developed with a nozzle temperature of 200 °C, a bed temperature of 60 °C in a high printing resolution set up with a layer height of 0.1 mm, the top thickness of 1 mm, infill density of 25%, infill speed of 35 mm/s, outer wall speed 20 mm/s, inner wall speed 25 mm/s, and a travel speed of 40 mm/s. Each piece of paper was fixed on the bed of the 3D printer using double-sided adhesive tabs (Ted Pella, Inc.) in the corners.

2.3. Wax curing process

High-temperature curing process allowed the wax on the paper to melt and penetrate the fibers of the different papers to create the hydrophobic barrier. For the curing process, a laboratory oven was used at different temperatures depending on the experiments described in each test. While the curing process may be done on a hot plate, heat does not produce consistent results. Therefore, a laboratory oven was used, which proved to be highly consistent.

2.4. Electrochemical measurements

A Gamry Reference 600+ Potentiostat was used for all electrochemical experiments. All electrochemical experiments were performed using a two-electrode system with one of the electrodes as the working electrode and the other electrode as the reference and counter electrode. The electrodes used are interdigital silver inkjet electrodes designed in AutoCAD Academic software. These interdigital electrodes have 13 finger-like structures that interlock with each other without touching. Each finger is 4.5 mm long and 400 μm wide. The total area of each interdigital silver inkjet electrode is 10 mm long and 5 mm wide. These electrodes were printed on the surface of the PET and glossy paper sheets using an Epson m1170 inkjet printer with silver nanoparticles ink from Novacentrix, Inc. To electrochemically characterize the inkjet-printed silver microelectrodes, cyclic voltammetry was performed at a potential window of –0.6 to 0.6 V at a scan rate of 50 mV/s in a two-electrode configuration where one of the interdigital electrodes is the working electrode, and the other electrode is the reference and counter electrode.

3. Results and discussion

3.1. µPADS fabrication in different types of paper

One of the advantages of using 3D printers for paper-based microfluidics is that µPADS can be fabricated on different paper types and is not limited to papers that can fit into a typical Xerox printer. Moreover, the design and fabrication are determined by the 3D printer used, for which there is an extensive community for custom modifications. Although it is possible to fabricate µPADS on different types of paper, it is necessary to determine the optimal paper that can provide a controlled passive flow. Another important factor is that the wax can be thermally cured on its surface, penetrating the fibers of the paper's surface without any problem. We tested three types of paper material to determine which is best for manufacturing microfluidic channels based on paper and wax filament. We used delicate task wipes (Kimwipes®), hard wound paper towels, and chromatography paper grade 1. Fig. 1A shows printed wax circles after the curing process on a Kimwipe®. The curing process was carried out in an oven at a temperature of 200 °C for 5 min. Since Kimwipes® are less thick than the other two types of papers tested, the deposited wax was able to penetrate much faster. One drop of water was applied to each of the wax circles after the high-temperature curing process to test the hydrophobic barrier of the applied wax. Fig. 1A (0 min) shows the moment after the green-dyed water was applied to the delicate task paper, and Fig. 1A (15 min) shows the same paper after 15 min of the wax circle being exposed to green-dyed water, demonstrating the good penetration of the wax on the paper after the curing process. All tested wax circles were able to retain water within the hydrophobic barrier. Fig. 1B shows the same test applied to hard wound paper towel. As with delicate task wipes, a series of circles were designed and printed on the surface of a paper towel. Fig. 1B shows the same circles from previous tests printed on hard wound paper towels after the curing process, where full penetration of the wax through the paper was observed. The curing process was carried out also at 200 °C in a laboratory oven for 5 min. Similarly, Fig. 1B (0 min) and (15 min) show the paper towel green-dyed water test results. After 15 min, all the circles retained the green-dyed water drop in the center of the hydrophobic wax barrier without spillage. This was constantly seen for all types of papers tested without any spillage during the time that was tested. Fig. 1C shows the same test applied to chromatography paper grade 1 with similar results obtained, where green-dyed water was retained within the wax circle after 15 min due to the hydrophobic barrier made by cured wax.

In Fig. 2A, a scanning electron microscopy (SEM) image is shown that was taken of a transversal cut in a piece of Kimwipe (between dashed blue lines) with a wax line (dashed red oval) printed on its surface without the curing process. We can see in the image how the wax line is just above the paper fibers (dashed red oval). In Fig. 2B, an SEM image of the internal structure of a transversal cut of Kimwipe with the wax line after the curing process is shown, and where the wax covers the fibers of the Kim wipes paper completely. Fibers can be seen mixed and in contact with the wax across the entire image. Blue arrows show areas with wax and red arrows show the fibers that are within and embedded on the wax forming a hydrophobic barrier.

Kimwipes and hard wound paper towels were chosen as they are very absorbent paper types; however, the capillary flow is not characterized and standardized as in chromatography paper. Paper towels were used for our proof-of-concept due to their fast flow of water due to capillarity, which made them better to test the hydrophobic barriers in thin (Kimwipes) and thick (hard wound paper towel) papers. Therefore, we proceeded with a standard paper after proof-of-concept testing of our developed 3D printing wax method and curing process on absorbent papers. We used chromatography paper grade 1 for the characterization and optimization of the paper-based microfluidic manufacturing method for biosensing since the passive flow on the surface of chromatography paper is much more controlled than typical absorbent paper towels.

3.2. Chromatography paper µPADs characterization

Fig. 2C and D show SEM images of chromatography paper type 1 before and after 3D wax printing and curing. Paper is composed of several cellulose fibers that form porosities in the structure of the paper. Fig. 2C shows the porosities of the fibers in the chromatography paper without the wax. The fibers of the paper and the pores or cavities formed between these cellulose fibers produce a very controlled flow of solution through the paper. After wax printing and curing, Fig. 2D shows the internal structure of the chromatography paper with a wax covering the fibers and pores of the paper, forming an excellent hydrophobic barrier.

3.3. Optimization of 3D printing conditions

To determine the minimum width of the hydrophobic barrier that can be used for printing, we first designed several circles in Fusion 360 extruded from 0.15 mm to 1.0 mm of wall width. Each circle was created with the same nozzle and offset measurement to determine the limit of our specific 3D printer (Snapmaker 1.0). In Fusion 360 software, there are no dimension limits for creating designs or patterns; however, the 3D printer software has minimum limits on printing dimensions depending on the type of printer. We could confirm that the minimum width generated for a design or pattern was 0.40 mm in our case due to nozzle size. To determine the minimum thickness that the 3D printer could print, a series of circles was designed, all with a 0.40 mm width, and the thickness in each circle was from 0.10 mm to 0.50 mm. In Fig. S1, the designs of the different circles are used for testing. Determining the minimum printing was essential to avoid depositing too much wax on the paper because expanding the wax on the paper during the curing process reduces the channel size. For microfluidics on paper, the amount of material deposited to create the hydrophobic barrier should be enough to penetrate the entire paper thickness while avoiding over deposition to decrease the channel size or the design of interest. In this work, we optimized our system for our 3D printer and decided to run all the experiments shown with a thickness of 0.15 mm and a width of 0.40 mm.

3.4. Wax expansion after curing

In paper-based microfluidics, the expansion of the wax on the surface of the paper after the curing process must be considered in the fabricated material. This expansion occurs when the wax is printed and cured at a high temperature on the paper surface due to the wetting process of the wax on the fibers. The wax expansion once the curing process is finished

must be considered so that the wax can finish penetrating throughout the paper and form the hydrophobic barrier while not moving sideways so much that it blocks the channel. The first expansion is due to the temperature at which the wax is printed on the surface. To deposit wax by extrusion on the surface of a paper, it is necessary to bring the wax to a temperature where it can melt. Although this first expansion is not as significant as the expansion after curing, the amount of material can affect the final channel. It is important to make prints with the minimum required material to avoid more significant expansions that may affect the dimensions of the patterns, channels, or designs while reaching the entire thickness of the paper during curing. To study the wax's expansion on the chromatographic paper's surface, we designed a series of microfluidic channels 10 mm long, a channel width of 4 mm, and wax lines in different widths from 0.50 to 1.00 mm. This test was performed in different conditions better to understand the expansion of the wax during printing and curing for a total of 20 times at different temperatures (200 °C, 225 °C, 250 °C) and curing times (5 min, 10 min, 15 min, 20 min). The wax line width was measured from each channel before and after the curing process and channel width. Fig. 3 shows how the expansion in the 3D printing and curing process affects the dimensions of the channels. After printing, it is clear that while the designed channel had a width of 4 mm, the measurements are smaller due to the expansion produced during wax extrusion in the 3D printer that must be considered in the design. Moreover, once the curing process is complete, the expansion of the lines increases more than twice the designed width in every case. The channel width decreases to almost half the size after the curing process. A significant change was observed in the expansion of the wax comparing the channels with lines from 0.50 mm to 1.00 mm in width. However, a small change is seen in the width of the channel due to the initial wax line width.

3.5. Resolution barrier test

To determine the 3D printing resolution, we performed a barrier test. In this test, we designed circles with line widths from 0.40 mm to 1.00 mm to observe their capacity to retain the water within the circles. All circles have a size of 8 mm in diameter, a line thickness of 0.15 mm, and outer circles of 15 mm in diameter, with line widths of 1.00 mm, which serve as a barrier in case any test circle was not able to retain the liquid. In Fig. S2, the barrier resolution test results with all the circles filled with a green dye solution. All circles managed to keep the green dye solution within their wax barriers. These results indicate that we can make hydrophobic barriers up to the minimum printing (0.40 mm line width) of this 3D printer.

3.6. Channel width/passive flow test

One of the applications of paper-based microfluidics is to manufacture microfluidic channels that can promote a passive and controlled flow. A test with different widths of microfluidic channels was performed, from 1.5 mm to 5 mm wide. Before conducting the passive flow test, it is necessary to ensure that the wax has completely penetrated the chromatography paper after the curing process. 50 μL of green-dyed water was added to each channel to measure the flow. Fig. 4 shows that the 2.5 mm to 5.0 mm channels had no problem with the flow path. Channels with widths of 1.5 and 2.0 mm did not allow the flow to reach the end of the channel. This was due to the expansion of the wax on the chromatography paper after the curing process, decreasing the width of the channels. These results are consistent with

the data obtained in the wax expansion test, where an expansion of the wax can be observed after the curing process, which affects the size of the channel. All channels designed with a width from 2.5 to 5.0 mm had a similar flow rate.

3.8. μPADs application for flexible biosensors

The electrodes must constantly contact the microfluidic channel flow to obtain the best possible detection. This can be accomplished by thermally bonding the planar electrodes to the wax and paper-based microfluidic channel arrangement. With this method of manufacturing paper-based microfluidics, it is possible to adhere inkjet-printed electrodes to the surface of a paper-based microfluidic with wax. Once the wax curing process is carried out on the surface of the chromatography paper, the electrodes are quickly placed in the microfluidic channel and then heated for 2 min at 200 °C. As a result, the PET-printed electrodes stuck to lines of wax that are still melting. Once cooled to room temperature, the inkjet electrode stayed in contact with the microfluidic channel. This process created a seal that did not allow the flow to leave the microfluidic channel once it reached the electrode array area. Therefore, this allowed us to use our developed wax-based microfluidic channels as a passive flow microfluidic for flexible biosensors. Fig. 5A and 5B are the setups for measuring the inkjet-printed microelectrodes on PET and glossy paper substrates, respectively. With these two prototypes, we aimed to characterize both substrates bonded to the wax-based microfluidic for electrochemical measurements on PET and Glossy paper and compare the peak currents of these electrodes using paper-based microfluidics as passive flow. This microfluidic design has a circular inlet, a microfluidic channel where electrodes are placed for analysis, and a waste reservoir. 50 μL were added to each one at the inlet of a tris buffer at 7.4 pH. In Fig. 5C, the voltammograms obtained from the flexible biosensors with inkjet electrodes printed on PET and Glossy paper are observed. Even though the design and print of the silver microelectrodes were the same, the PET-based microelectrodes obtained almost double the anodic and cathodic current compared to the paper-based microelectrodes. These results can be confirmed through electrochemical impedance spectroscopy at 0.0 V, as seen in Fig. 5D, where charge transfer resistance is smaller in PET-based microelectrodes characterized by the smaller semi-circle obtained compared to paper-based microelectrodes.

3.9. Electrochemical μPAD application in dopamine measurement

One of the applications of microfluidics is using them as a passive flow movement method in developing flexible electrochemical biosensors. Paper-based flexible biosensors are a new generation of point-of-care diagnostic devices that integrate microfluidics as a flexible and simple technology that uses a passive flow [22–24]. Due to the complexity of operational principles and the manufacture of wearable chemical sensors, paper-based colorimetric assays are the most common and widely developed since they are the best option for some applications. However, electrochemical sensing provides better versatility and quantitative methodology [25,26].To test the applicability of μPADS manufacturing, we performed measurements of dopamine concentrations in constant flow through chronoamperometry, using PET-based inkjet-printed interdigital silver electrodes thermally cured in paper-based microfluidics with wax. We decided to use PET-based microelectrodes because they had higher electrical currents and were more stable in contact with water for long periods.

15 μL of PBS buffer at 7.4 pH and different dopamine concentrations were applied to the microfluidic system with inkjet-printed microelectrodes in concentrations of 1 nM, 5 nM, 10 nM, and 25 nM. The concentrations were applied from lowest to highest and measured by chronoamperometry at a constant potential of 0.1 V in a two-electrode system. For each concentration, three quantities of 15 μL were injected into the inlet of the paper-based microfluidic device. In Fig. 6A, the chronoamperometry of different dopamine concentrations is shown where three peaks for each dopamine concentration can be seen. The peak current and area increase can be seen as the dopamine concentration increases. However, in the last three peaks corresponding to the 25 nM dopamine concentration, there is no increase in the peak current and area compared to the 10 nM dopamine concentration. The area under the peaks was plotted versus dopamine concentrations to establish a relationship between the increase in dopamine concentration and the peak area. Fig. 6B shows the relationship between the increase in concentration and peak area with saturation at a dopamine concentration of 10 nM. This may be due to the polymerization of dopamine on the surface of the working microelectrodes after several dopamine injections into the μPAD. These results proved the use of our μPADS manufacturing method for developing and manufacturing portable electrochemical flexible biosensors with a passive flow movement.

4. Conclusion

We developed a method of manufacturing paper-based microfluidics using a commercial 3D printer, wax filament, and chromatography paper. After printing, paper-based microfluidic is placed in an oven to carry out a thermal process so the wax can penetrate the fibers of the chromatography paper to form a hydrophobic barrier. This paper-based microfluidic manufacturing method is easy, affordable, low-cost to produce, and fast compared to today's traditional methods for paper-based microfluidic manufacturing. Additionally, this method provides an alternative for those still relying on wax printers already discontinued by manufacturers. Using a commercial 3D printer, we made wax prints at a minimum resolution with lines 0.15 mm high and 0.40 mm wide. Moreover, the 3D print resolution can be increased by changing nozzle size and printing speed. Finally, we manufactured a μPAD with a silver interdigitated array sealed in contact with the channel. Using this system, we measured dopamine using chronoamperometry in concentrations as low as 1 nM with injections as small as 15 μL. This proof-of-concept opens the door to the use of the limitless technology of 3D printing for manufacturing paper-based microfluidics using wax.

Supplementary Material

Refer to Web version on PubMed Central for supplementary material.

Acknowledgments

References

[1]. Liu KK, Wu RG, Chuang YJ, Khoo HS, Huang SH, Tseng FG, Microfluidic systems for biosensing, Sensors 10 (2010) 6623–6661, 10.3390/s100706623. [PubMed: 22163570]

[2]. Yew M, Ren Y, Koh KS, Sun C, Snape C, A review of state-of-the-art microfluidic technologies for environmental applications: detection and remediation, Glob. Chall 3 (2019), 1800060, 10.1002/gch2.201800060. [PubMed: 31565355]

[3]. Altundemir S, Uguz AK, Ulgen K, A review on wax printed microfluidic paper-based devices for international health, Biomicrofluidics 11 (2017), 041501, 10.1063/1.4991504. [PubMed: 28936274]

[4]. Tseng CC, Kung CT, Chen RF, Tsai MH, Chao HR, Wang YN, Fu LM, Recent advances in microfluidic paper-based assay devices for diagnosing human diseases using saliva, tears, and sweat samples, Sens. Actuators B 342 (2021), 130078, 10.1016/j.snb.2021.130078.

[5]. Choi S, Kim SK, Lee GJ, Park HK, Paper-based 3D microfluidic device for multiple bioassays, Sens. Actuators B 219 (2015) 245–250, 10.1016/j.snb.2015.05.035.

[6]. Soum V, Park S, Brilian AI, Kwon OS, Shin K, Programmable paper-based microfluidic devices for biomarker detections, Micromachines (Basel) 10 (2019), 10.3390/mi10080516.

[7]. Channon RB, Nguyen MP, Scorzelli AG, Henry EM, Volckens J, Dandy DS, Henry CS, Rapid flow in multilayer microfluidic paper-based analytical devices, Lab Chip 18 (2018) 793–802, 10.1039/c7lc01300k. [PubMed: 29431751]

[8]. Sinha A, Basu M, Chandna P, Paper-based microfluidics: a forecast toward the most affordable and rapid point-of-care devices. Progress in Molecular Biology and Translational Science, Academic Press, 2021.

[9]. Boobphahom S, Ly MN, Soum V, Pyun N, Kwon OS, Rodthongkum N, Shin K, Recent advances in microfluidic paper-based analytical devices toward high-throughput screening, Molecules 25 (2020), 10.3390/molecules25132970.

[10]. Tseng CC, Kung CT, Chen RF, Tsai MH, Chao HR, Wang YN, Fu LM, Recent advances in microfluidic paper-based assay devices for diagnosing human diseases using saliva, tears, and sweat samples, Sens. Actuators B 342 (2021), 130078, 10.1016/j.snb.2021.130078.

[11]. Noviana E, McCord CP, Clark KM, Jang I, Henry CS, Electrochemical paper-based devices: sensing approaches and progress toward practical applications, Lab Chip 20 (2020) 9–34, 10.1039/c9lc00903e. [PubMed: 31620764]

[12]. Morbioli GG, Speller NC, Cato ME, Cantrell TP, Stockton AM, Rapid and low-cost development of microfluidic devices using wax printing and microwave treatment, Sens. Actuators B 284 (2019) 650–656, 10.1016/j.snb.2018.12.053.

[13]. Younas M, Maryam A, Khan M, Nawaz AA, Jeffery SHI, Anwar MN, Ali L, Parametric analysis of wax printing technique for fabricating microfluidic paper-based analytic devices (μPAD) for milk adulteration analysis, Microfluid. Nanofluidics 23 (2019) 38, 10.1007/s10404-019-2208-z.

[14]. Nilghaz A, Liu X, Ma L, Huang Q, Lu X, Development of fabric-based microfluidic devices by wax printing, Cellulose 26 (2019) 3589–3599, 10.1007/s10570-019-02317-z.

[15]. Chiang CK, Kurniawan A, Kao CY, Wang MJ, Single-step and mask-free 3D wax printing of microfluidic paper-based analytical devices for glucose and nitrite assays, Talanta 194 (2019) 837–845, 10.1016/j.talanta.2018.10.104. [PubMed: 30609613]

[16]. Kim JH, Mun S, Ko HU, Yun GY, Kim J, Disposable chemical sensors and biosensors made on cellulose paper, Nanotechnology 25 (2014), 092001, 10.1088/0957-4484/25/9/092001. [PubMed: 24521757]

[17]. Tortorich R, Shamkhalichenar H, Choi JW, Inkjet-printed and paper-based electrochemical sensors, Appl. Sci 8 (2018) 288, 10.3390/app8020288.

[18]. Steckl AJ, Ray P, Stress biomarkers in biological fluids and their point-of-use detection, ACS Sens. 3 (2018) 2025–2044, 10.1021/acssensors.8b00726. [PubMed: 30264989]

[19]. Johnson JA, Rodeberg NT, Wightman RM, Measurement of basal neurotransmitter levels using convolution-based nonfaradaic current removal, Anal. Chem 90 (2018) 7181–7189, 10.1021/acs.analchem.7b04682. [PubMed: 29806450]

[20]. Rivera-Serrano N, Pagan M, Colón-Rodríguez J, Fuster C, Vélez R, Almodovar-Faria J, Jiménez-Rivera C, Cunci L, Static and dynamic measurement of dopamine adsorption in carbon fiber microelectrodes using electrochemical impedance spectroscopy, Anal. Chem 90 (2018) 2293–2301, 10.1021/acs.analchem.7b04692. [PubMed: 29260558]

[21]. Lei Y, Butler D, Lucking MC, Zhang F, Xia T, Fujisawa K, Granzier-Nakajima T, Cruz-Silva R, Endo M, Terrones H, Terrones M, Ebrahimi A, Single-atom doping of MoS2 with manganese enables ultrasensitive detection of dopamine: experimental and computational approach, Sci. Adv 6 (2020), eabc4250, 10.1126/sciadv.abc4250. [PubMed: 32821846]

[22]. Liu B, Du D, Hua X, Yu XY, Lin Y, Paper-based electrochemical biosensors: from test strips to paper-based microfluidics, Electroanalysis 26 (2014) 1214–1223, 10.1002/elan.201400036.

[23]. Kim S, Kim D, Kim S, Multiplexed detection of biomolecules using a wax printed paper-disc centrifugal optical device, Sens. Actuators B 303 (2020), 127195, 10.1016/j.snb.2019.127195.

[24]. Juang YJ, Chen PS, Wang Y, Rapid fabrication of microfluidic paper-based analytical devices by microembossing, Sens. Actuators B 283 (2019) 87–92, 10.1016/j.snb.2018.12.004.

[25]. Cao Q, Liang B, Tu T, Wei J, Fang L, Ye X, Three-dimensional paper-based microfluidic electrochemical integrated devices (3D-PMED) for wearable electrochemical glucose detection, RSC Adv. 9 (2019) 5674–5681, 10.1039/C8RA09157A. [PubMed: 35515907]

[26]. Nie Z, Nijhuis CA, Gong J, Chen X, Kumachev A, Martinez AW, Narovlyansky M, Whitesides GM, Electrochemical sensing in paper-based microfluidic devices, Lab Chip 10 (2010) 477–483, 10.1039/b917150a. [PubMed: 20126688]
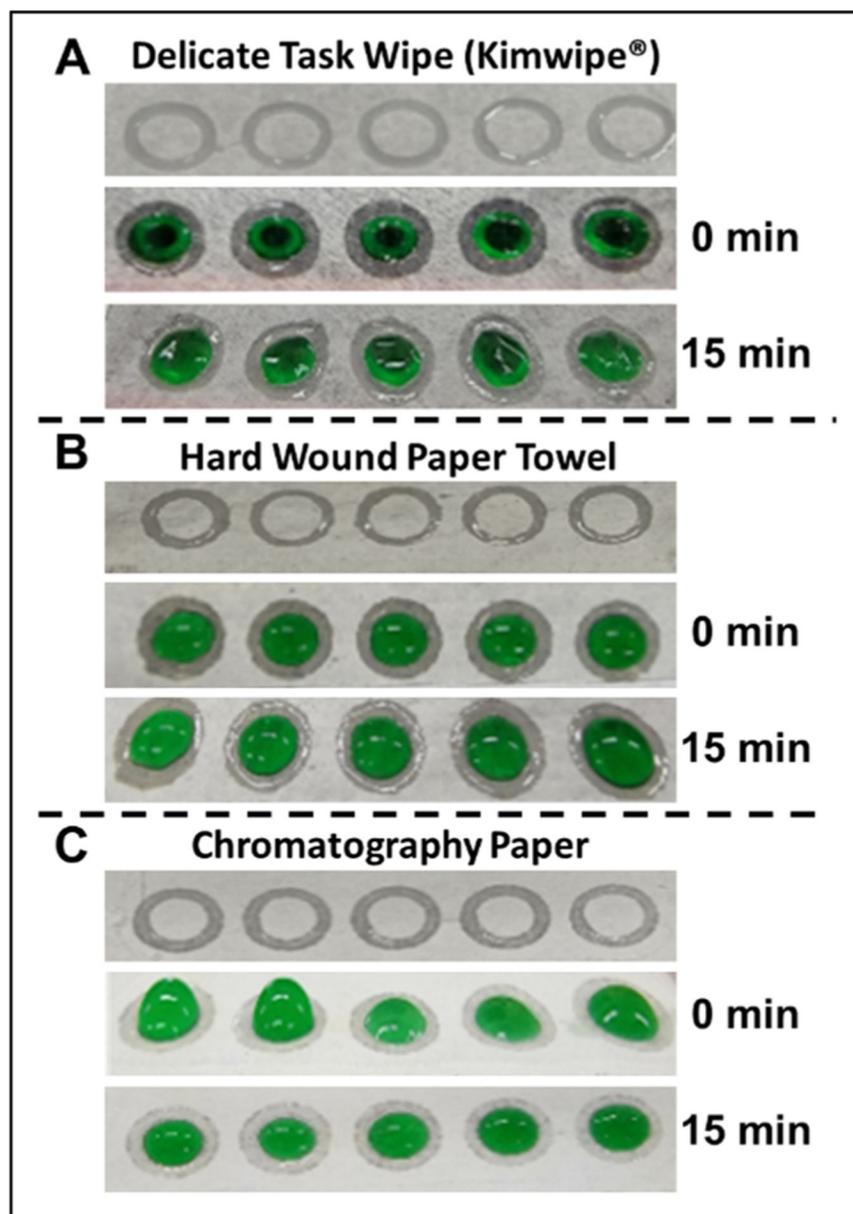
Fig. 1.
Wax circles cured on a (A) Kimwipe®, (B) hard wound paper towel, and (C) chromatography paper at 200 °C for 5 min (0 min) before the green-dyed water application, and (15 min) after 15 min showing the green-dyed water retention due to the hydrophobic barrier formed by the wax.
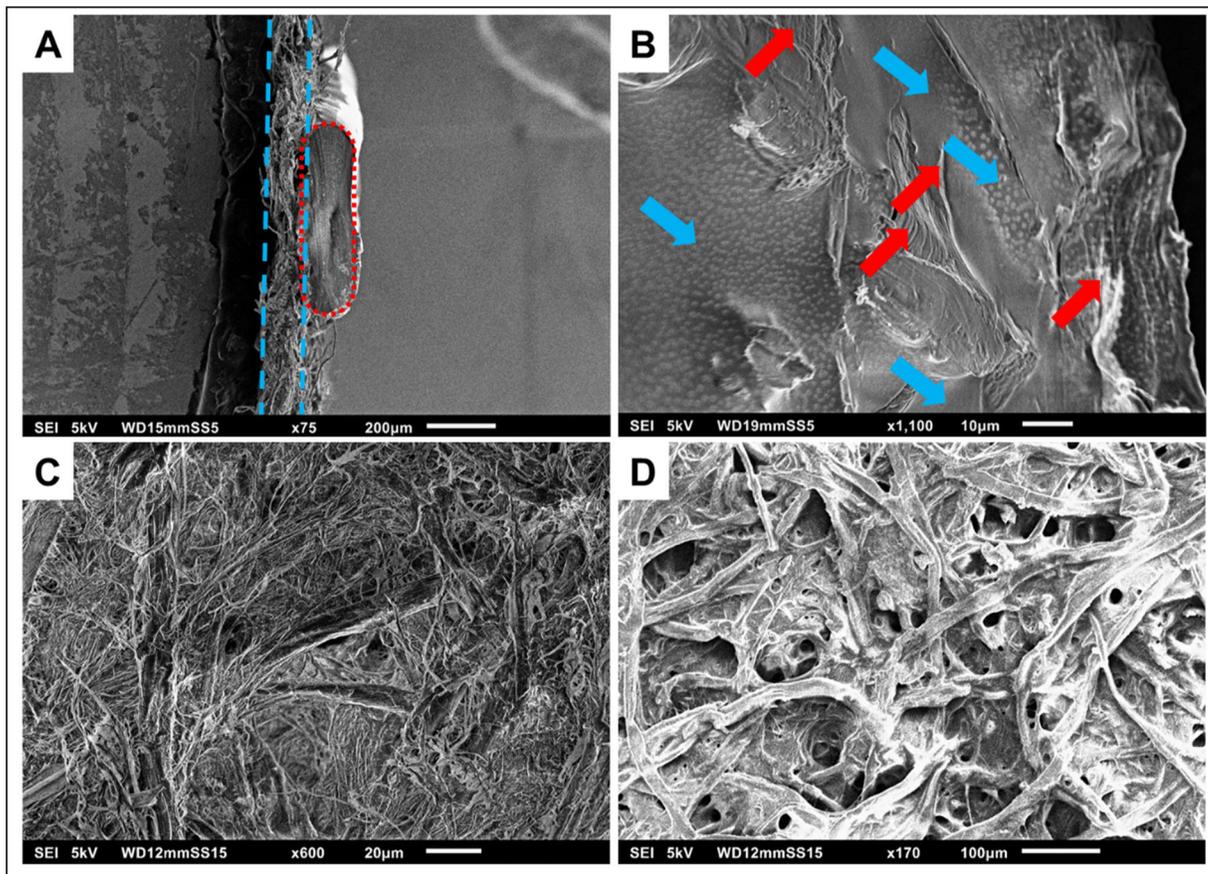
Fig. 2.
A scanning electron microscopy image taken of a piece of a delicate task paper (between the dashed blue lines) with a wax line (dashed red oval) printed on its surface (A) before and (B) after the curing process. Blue arrows show areas with wax and red arrows show the fibers that are within and embedded on the wax forming a hydrophobic barrier. Before the curing process, the fibers and wax are separated, and after the curing process the internal structure shows a mix of fibers with wax. (C) Scanning electron microscopy images of chromatography paper before wax printing and curing showing the fibers and porosity that make up the paper. (D) Scanning electron microscopy image of the same chromatography paper after the wax printing and curing process showing how the wax covers the paper fibers and covers the pores, creating a hydrophobic barrier.
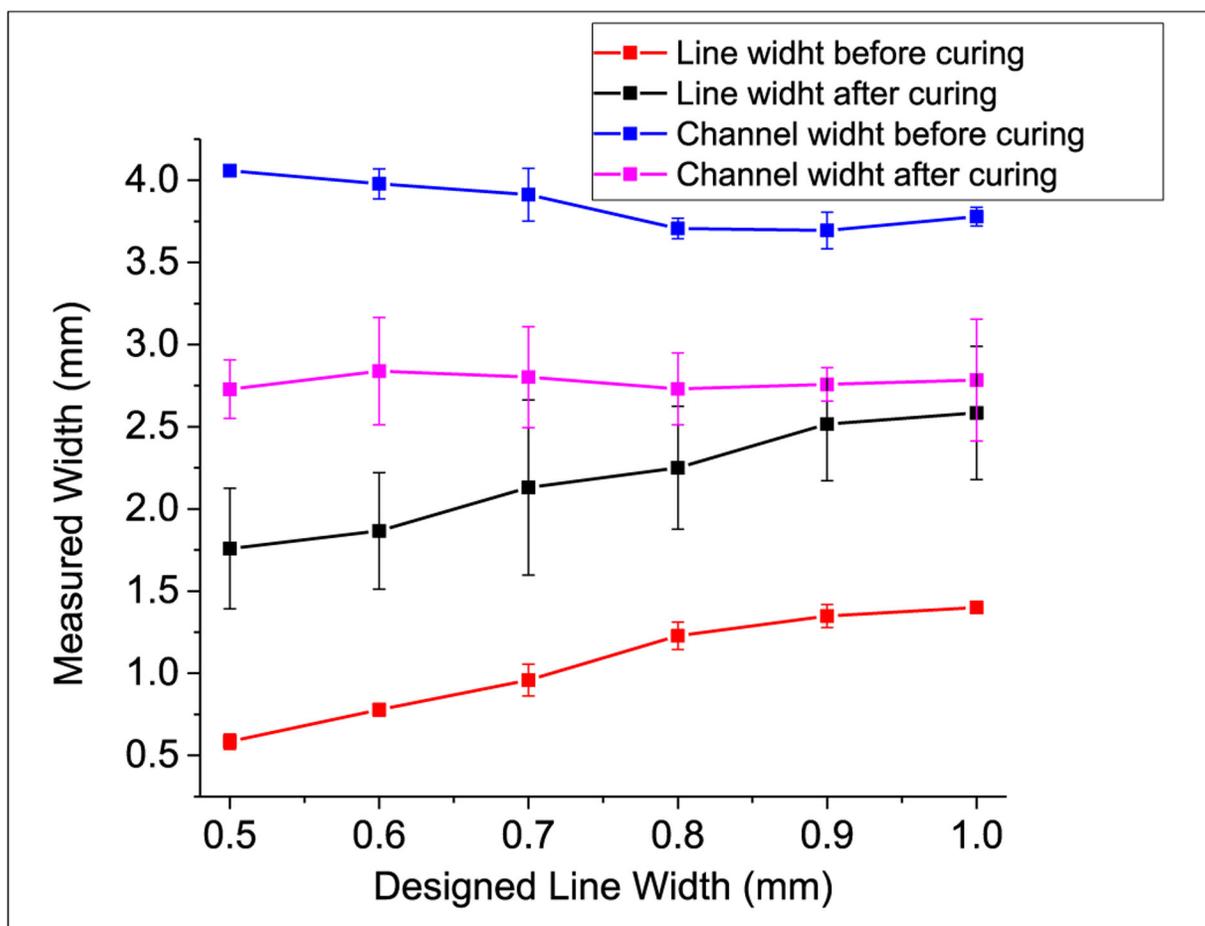
Fig. 3.
The measured wax line and channel width before and after the high-temperature curing
process compared to the theoretical width of the wax in the design. Data points represent the
mean of $n = 6$, and error bars represent standard deviations from the mean.
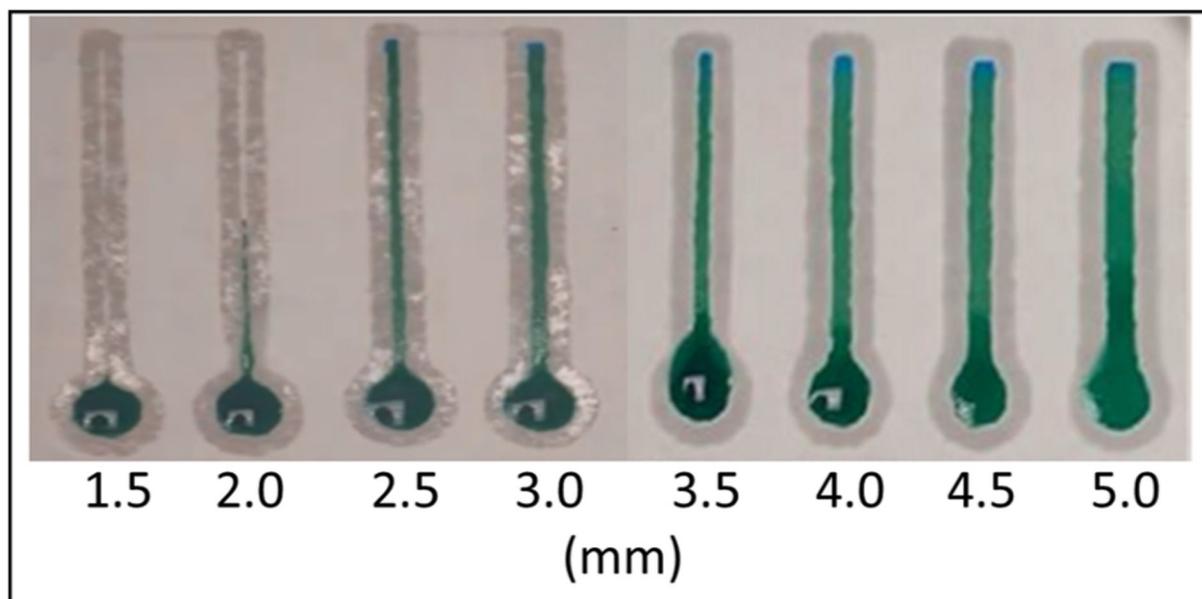
Fig. 4.
Test with different designed widths of microfluid channels from 1.5 mm to 5.0 mm. Each track was filled with 50 μL of a green ink solution to measure its flow.
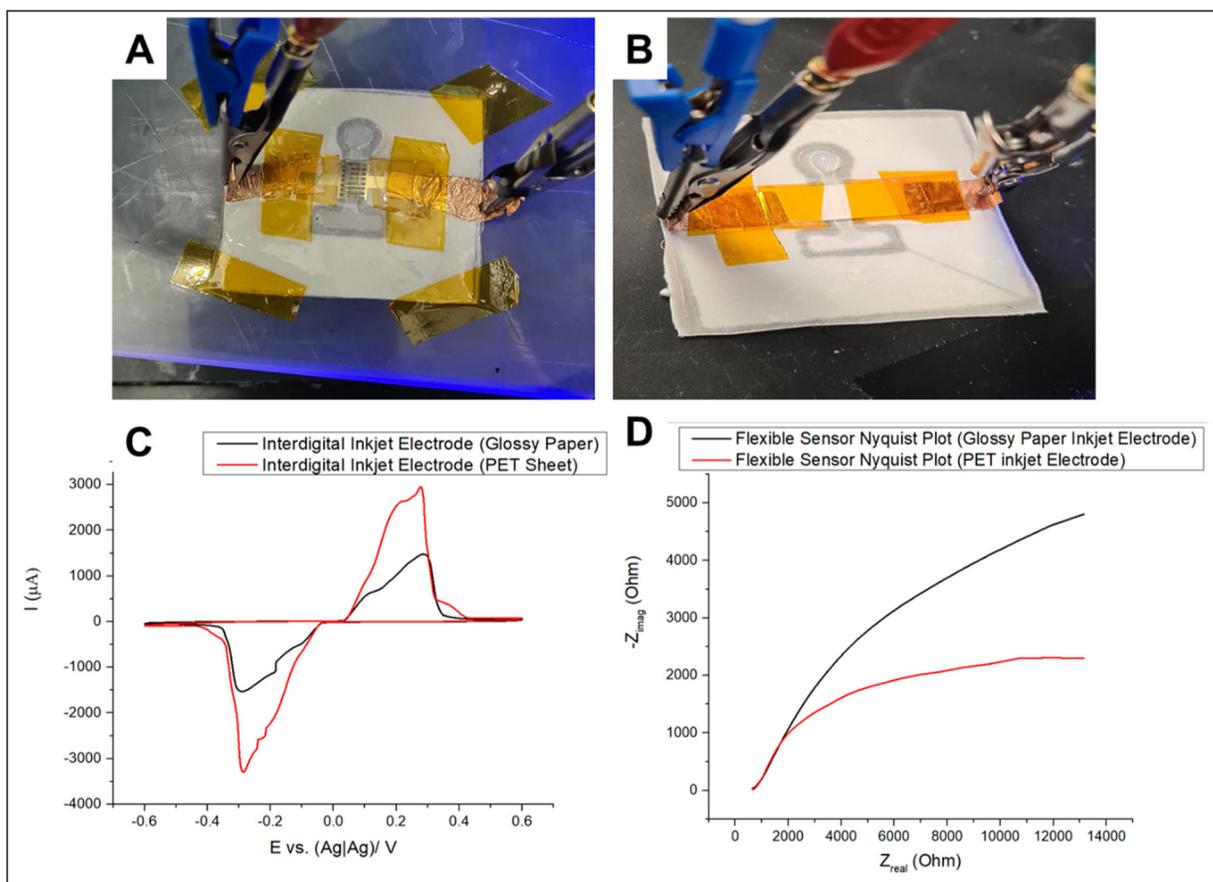
Fig. 5.
Flexible biosensor prototypes with interdigital silver microelectrodes inkjet-printed on (A) PET and (B) glossy paper for electrochemical characterization. (C) Cyclic voltammetry was obtained from flexible biosensors using a tris buffer with a 7.4 pH. (D) Electrochemical impedance spectroscopy experiment showing the Nyquist plot obtained at 0.0 V. All electrochemical experiments were done in a two-electrode system using one electrode as a working electrode and the other electrode as a reference and counter electrode.
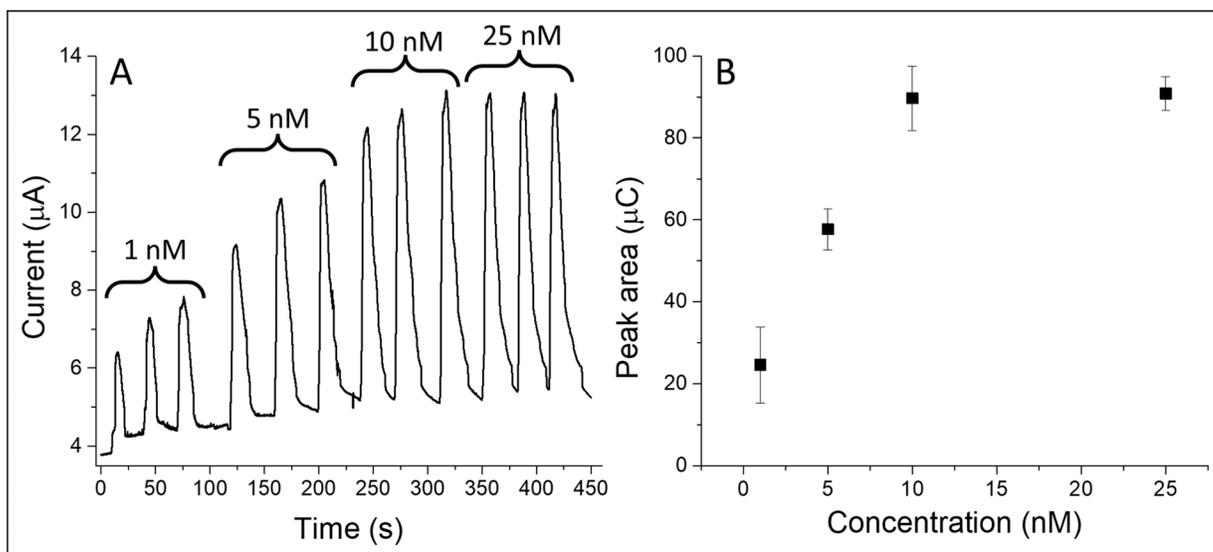
Fig. 6.
(A) Chronoamperometry result of dopamine concentrations of 1 nM, 5 nM, 10 nM, and 25 nM in a paper-based microfluidic sensor at constant flow and the (B) relationship between the change of the peak area and the dopamine concentration. Data points represent the mean of $n = 3$, and error bars represent standard deviations from the mean.